

Structure-Based Identification of Novel Human γ -Glutamylcysteine Synthetase Inhibitors

David Hamilton, Jian Hui Wu, and Gerald Batist

Departments of Oncology, Pharmacology and Therapeutics, McGill University, Montreal Centre for Experimental Therapeutics in Cancer and Segal Cancer Centre, Lady Davis Institute for Medical Research, Sir Mortimer B. Davis-Jewish General Hospital, Montreal, Quebec, Canada

Received March 21, 2006; accepted January 17, 2007

ABSTRACT

Glutathione depletion represents a potentially important strategy to sensitize tumors to cytotoxic drugs. L-Buthionine-(*R,S*)-sulfoximine (L-BSO) has been studied in both preclinical and early clinical trials, but limitation on its access has led to a search for alternatives. Using a 3D molecular model of human γ -glutamylcysteine synthetase (γ -GCS_H), the major subunit of the rate-limiting GSH synthetic enzyme, we virtually screened the National Cancer Institute chemical database to identify compounds that could bind to and potentially inhibit γ -GCS_H.

We identified 51 test chemicals, all with structures very distinct from L-BSO. We subjected these compounds to biological assays measuring γ -GCS_H inhibition and glutathione (GSH) depletion. Among 10 novel γ -GCS inhibitors identified, 4 compounds depleted glutathione in cells, and 2 with related structures sensitized tumor cells to melphalan treatment. This work validates the use of model-based database mining and identified inhibitors of γ -GCS_H with novel chemical structures.

Glutathione (L- γ -glutamyl-L-cysteinyl-glycine; GSH) is an intracellular tripeptide antioxidant that plays an important role in the maintenance of cellular redox potential and also functions in many other biological processes such as protein and DNA synthesis; detoxification of free radicals, peroxides, and endogenous and exogenous toxins; and amino acid transport (Meister and Anderson, 1983; Meister, 1989). The heterodimeric enzyme γ -glutamylcysteine synthetase (γ -GCS) is composed of heavy (γ -GCS_H, 637 amino acid) and light (γ -GCS_L, 274 amino acid) subunits and catalyzes the first and rate-limiting reaction in GSH biosynthesis. γ -GCS_H exhibits all the catalytic activity of the native enzyme and is also the site of feedback inhibition by GSH, whereas γ -GCS_L plays an important regulatory role by increasing substrate affinity. Elevated levels of GSH have been implicated in cellular resistance to alkylating agents, platinum compounds, and irradiation (Griffith and Friedman, 1991). In particular, relative elevations of GSH and γ -GCS have been strongly associated with drug resistance in ovarian tumor cells (Lewandowicz et al., 2002). Depletion of GSH by

L-buthionine-(*R,S*)-sulfoximine (L-BSO) (1, Fig. 1), a potent inhibitor of γ -GCS, can reverse drug resistance in these same cells. More recently, GSH and cellular antioxidant capacity have been linked to cellular resistance to topoisomerase inhibitors and to taxanes (Ramanathan et al., 2005; Yoshida et al., 2006). Redox active or generating reagents such as arsenic trioxide have been shown to have enhanced cell killing in the presence of GSH depletion by L-BSO (Zhu et al., 1999; Davison et al., 2004).

Other data suggest that GSH not only functions in a redox capacity in drug resistance but also conjugates some drugs and renders them substrates for efflux pumps. Rappa et al. (2003) showed that MRP1-overexpressing cells were hypersensitive to L-BSO, which has provided a new rationale for the use of γ -GCS inhibitors in the treatment of MRP1-overexpressing tumors (Rappa et al., 2003). This was subsequently shown again in a kidney epithelial cell line engineered to overexpress MRP1 (Akan et al., 2005).

During a phase I clinical trial combining L-BSO and melphalan in heavily pretreated patients with ovarian cancer, investigators demonstrated that the treatment was effective at reducing tumor GSH levels and produced clinical responses in a limited number of patients who were previously refractory (Dwyer et al., 1996), supporting the view that GSH modulation may represent a novel and effective therapeutic strategy. Preliminary data from a phase II trial of melphalan

This work was supported by Canadian Institute of Health Research via operating grants (to G.B. and J.H.W.) and by the Réseau de recherche sur le cancer, Fonds de la recherche en santé du Québec.

Article, publication date, and citation information can be found at <http://molpharm.aspetjournals.org>.
doi:10.1124/mol.106.024778.

ABBREVIATIONS: GSH, glutathione; MRP1, multidrug resistance-related protein 1; L-BSO, L-buthionine-(*R,S*)-sulfoximine; γ -GCS_H, γ -glutamylcysteine synthetase; NCI, National Cancer Institute; DMSO, dimethyl sulfoxide.

plus L-BSO in the treatment of metastatic melanoma, performed by Batist et al., demonstrated greater inhibition of γ -GCS and greater depletion of GSH in the tumor compared with the normal peripheral mononuclear cells (Chen et al., 1998).

There have been difficulties in production and availability of L-BSO, in addition to its limited potency in GSH depletion, and these have stimulated a search for other molecules that can deplete GSH. To date, most studies of L-BSO analogs have focused on optimizing their potency against *Escherichia coli* γ -GCS (Fig. 1) (Griffith, 1982; Tokutake et al., 1998; Griffith and Mulcahy, 1999). Pentathionine sulfoximine and S-hexyl derivatives (2, Fig. 1) display an activity comparable with that of L-BSO but offer no advantage over L-BSO (Hiratake et al., 2002). Compound 3 is a much weaker inhibitor compared with L-BSO. In particular, compound 4, with R as ethyl, is a very potent inhibitor of *E. coli* γ -GCS, whereas compounds 5 and 6 are more potent than L-BSO in inhibiting *E. coli* enzyme (Tokutake et al., 1998; Hiratake et al., 2002). Moreover, all of the known γ -GCS inhibitors are effectively based on the L-BSO skeleton (Fig. 1) and vary in potency and toxicity. To continue clinical development of chemosensitizers that inhibit human γ -GCS for GSH depletion, it is desirable to identify novel chemical structures.

Virtual screening is a computational process in which a chemical library containing a large number of (available or virtual) compounds is mined against the three-dimensional (3D) structure of a target of interest to identify potential interactors. Numerous successful applications of virtual screening have been reported previously (Lyne, 2002). For example, in our previous work (Perola et al., 2000), a long-forgotten synthetic steroid derivative was identified as a microtubule-stabilizing agent. Because the crystal structure of mammalian γ -GCS_H has not been solved, it was necessary to build a structural model of human γ -GCS_H. We recently identified a novel γ -GCS_H hereditary mutation, R127C, in fibroblasts grown from two related patients diagnosed with γ -GCS deficiency, and that led us to generate a model of the putative active site of human γ -GCS_H (Hamilton et al., 2003). This provided us with the key tool necessary for the discovery of new inhibitors using virtual screening.

In this present study, we used our structural model to virtually screen the National Cancer Institute (NCI) 3D

chemical database for potential γ -GCS inhibitors. We adopted a multiple-cycle screening strategy that includes both receptor-based and ligand-based methods. Our main objective was to identify novel chemical classes of γ -GCS inhibitors. From 90,000 virtually screened compounds, 51 chemical candidates were physically obtained and subjected to enzymatic and cellular assays. This work led to the identification of four novel γ -GCS inhibitors that demonstrated activity in depleting cellular GSH and that possess chemical skeletons different from that of L-BSO. We also showed that GSH depletion resulted in sensitization to a cytotoxic alkylating antitumor agent.

Materials and Methods

Virtual Screening. The 3D structural model of γ -GCS_H was taken from our previous work (Hamilton et al., 2003). The open part of the NCI-3D database was processed using the Insight II package (Accelrys, Inc., San Diego, CA) with a script (Wu et al., 2001). To be exact, the counter-ions were stripped, hydrogen atoms were added, and atomic partial charges were assigned using the consistent-valence force field. Using the γ -GCS_H structural model, we virtually screened 90,000 compounds from the processed NCI-3D database using the software Genetic Optimization for Ligand Docking (GOLD) version 2.1 (The Cambridge Crystallographic Data Centre, Cambridge, UK), which is a genetic algorithm for calculating the docking modes of small molecules into protein binding sites. The ligand is treated as fully flexible, whereas the proteins were kept rigid except that each serine, threonine, and tyrosine hydroxyl group was allowed to rotate to optimize hydrogen bonding. GoldScore is the default scoring function of GOLD, and it was selected to give fitness score for each compound in this work. There are several optimized GOLD parameter settings that differ in the speed and accuracy for the docking studies: 1) the library screen setting is fast with reasonable accuracy, and 2) the standard setting is slower than the first one but gives more accurate predictions.

The three screening cycles and the overall results of the screenings were summarized by the flow charts in Fig. 2. In the first screening cycle, a data set of 90,000 NCI compounds was reduced to the top 800 compounds by the virtual screen using the GOLD library screen setting. This data set of 800 compounds was further reduced to 80 compounds using the GOLD standard setting. Among the 26 chemical samples subjected to enzymatic assays, 5 initial hits were identified. Next, we screened the NCI-3D database for the analogs of the five initial hits using the ANALOG algorithm that was developed locally and is based on a selected set of molecular descriptors. In

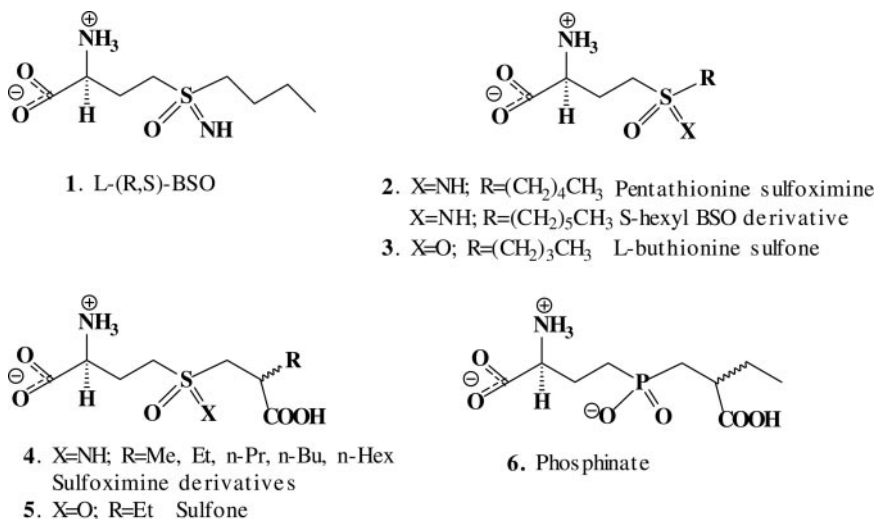


Fig. 1. Chemical structures of L-BSO and some of its analogs.

cycle 2, we identified 5 hits from the 22 analogs of the hits from the first cycle. In cycle 3, we identified two lead compounds from the analogs of the hits in cycle 2.

Enrichment curves are obtained by plotting the percentage of inhibitors retrieved as a function of the percentage of total molecules in the data set. The perfect selection curve (solid line) was plotted by assuming the 11 active compounds in the data set were ranked as 1 to 11. The random selection curves (Δ) are defined as the curve that the percentage of the active compounds retrieved is equal to the percentage of the database tested.

Chemicals. L-Buthionine sulfoximine [L-(R,S)-BSO], was purchased from Sigma (St. Louis, MO) and represents the same chiral form used in previous preclinical studies. The chemical samples of the NSC compounds were a gift from the Drug Synthesis and Chemistry Branch (Developmental Therapeutics Program, NCI, Bethesda, MD). To verify chemical structures of the NSC compounds, we performed ^1H NMR and mass spectrum analyses. The ^1H spectra were recorded on a Bruker AMX2 at 500 MHz (Bruker, Newark, DE). fast atom bombardment mass spectra were performed with a Quattro II (Micromass, Toronto, ON, Canada) mass spectrometer with a Z-spray interface, at unit resolution, and in the positive ion mode. The samples were dissolved in an acetonitrile/water mixture containing 1% acetic acid. The ^1H NMR spectra and mass spectrum analyses have confirmed the chemical structures of the active compounds (Table 1). The results are recorded as follows: NSC21429: ^1H NMR (CDCl_3) δ 1.42 (t, J = 7.1 Hz, 3H), 4.29 to 4.38 (m, 2H), 7.13 (d, J = 8.7 Hz, 1H), 7.18 (d, J = 8.8 Hz, 1H), 7.23 (s, 3H), 7.50 (d, J = 8.7 Hz, 1H), 7.79 (d, J = 8.8 Hz, 1H), 12.07 (s, 1H); MS 241, 242 [$\text{M} + \text{H}$] $^+$; NSC176282: ^1H NMR (CDCl_3) δ 1.43 (t, J = 7.1 Hz, 3H), 4.42 (q, J = 7.1 Hz, 2H), 7.37 (d, J = 8.1 Hz, 1H), 7.65 to 7.67 (m, 2H), 13.47 (s, 1H); MS 286, 287 [$\text{M} + \text{H}$] $^+$; NSC266746: ^1H NMR ($\text{DMSO}-d_6$) δ 4.03 (s, 2H), 7.29 to 7.32 (m, 1H), 7.36 to 7.40 (m, 4H), 7.69 (dd, J = 8.7, 2.6 Hz, 1H), 8.08 (s, 1H), 8.19 (br s, 1H), 8.34 (br s, 1H), 8.36 (d, J = 8.7 Hz, 1H), 8.41 (d, J = 2.6 Hz), 11.62 (s, 1H); MS 314, 315 [$\text{M} + \text{H}$] $^+$; NSC104960: ^1H NMR ($\text{DMSO}-d_6$) 1.37 (t, J = 6.7 Hz, 3H), 4.13 (q, J = 6.7 Hz, 2H), 7.37 (dd, J = 8.3, 4.4 Hz, 1H), 7.46 (br s, 1H), 7.52 (d, J = 8.3 Hz, 1H), 8.19 (d, J = 4.4 Hz, 1H), 8.29 (br s, 1H), 8.45 (s, 1H), 11.61 (s, 1H); MS 224, 225 [$\text{M} + \text{H}$] $^+$; NSC25809: ^1H NMR ($\text{DMSO}-d_6$) δ 3.93 (s, 3H), 7.34 (s, 1H), 7.73 (s, 2H), 8.01 (s, 1H), 13.0 (s, 1H); MS 228, 229 [$\text{M} + \text{H}$] $^+$; NSC118657: ^1H NMR (CDCl_3) δ 3.96 (s, 3H), 7.51 to 7.54 (m, 3H), 7.95 (d, J = 8 Hz, 4H), 8.20 (d, J = 8 Hz,

2H); MS 240, 241 [$\text{M} + \text{H}$] $^+$; NSC79068: ^1H NMR (CDCl_3) δ 1.30 (t, J = 7 Hz, 3H), 2.75 (q, J = 7 Hz, 2H), 7.37 (d, J = 8 Hz, 2H), 7.90 (d, J = 8 Hz, 2H), 7.96 (d, J = 8 Hz, 2H), 8.25 (d, J = 8 Hz, 2H); MS 254, 255 [$\text{M} + \text{H}$] $^+$; NSC59492: ^1H NMR (methanol- d_4) δ 2.45 (s, 3H), 7.38 (d, J = 8 Hz, 2H), 7.86 (d, J = 8 Hz, 2H), 7.94 (d, J = 8 Hz, 2H), 8.18 (d, J = 8 Hz, 2H); MS 240, 241 [$\text{M} + \text{H}$] $^+$; NSC24196: MS 236, 237 [$\text{M} + \text{H}$] $^+$, insoluble in chloroform, low solubility in either DMSO or *N,N*-dimethylformamide; and NSC299962: ^1H NMR (CDCl_3 , 500 MHz) δ 6.46 (s, 1H), 4.25 (q, 2H, J = 7.3 Hz), 3.65 (s, 2H), 2.32 (s, 1H), 2.16 (s, 3H), 2.08 (s, 3H), 1.32 (t, 3H, J = 7.3 Hz), MS 241, 242 [$\text{M} + \text{H}$] $^+$.

Cell Culture and Treatment. A549 cells were obtained from the American Type Culture Collection (Manassas, VA) and were cultured in minimal essential medium (Wisent, St. Bruno, QC, Canada) supplemented with nonessential amino acids, 10% fetal bovine serum, sodium pyruvate, and penicillin/streptomycin and maintained at 5% CO_2 and 37°C. A549 is an established lung cancer cell line, derived from a human non-small-cell lung cancer, has high levels of γ -GCS and GSH, and has been shown to express MRP1 protein in its cell membrane (Torky et al., 2005).

For each of the drugs, the highest nontoxic dose was determined (L-BSO, 100 μM ; NSC59492, 90 μM ; NSC79068, 100 μM). For each, the time to maximal GSH depletion was also determined, and in all cases, there was no greater depletion beyond 24 h, so that the subsequent studies with melphalan were performed using the respective GSH depleter at its highest nontoxic dose after 24 h of exposure. For cytotoxicity determination, cells (2×10^3) were seeded into 96-well plates and allowed to attach. The cells were then exposed to medium containing no addition, L-BSO, or the test molecules at the specified doses, for 24 h. Then the medium was changed and replaced with fresh medium containing the same addition (nothing, L-BSO, or test molecule), plus serial dilutions of melphalan and then were left in the incubator for 48 h, after which the medium was removed, the cells were fixed, and protein was stained using the sulforhodamine blue assay. Absorbance was read at 490 nm using an ELX800 microplate reader (Bio-Tek Instruments Inc., Winooski, VT). As control, nontreated DMSO- and L-BSO-treated cells were used. We used Prism (GraphPad Software Inc., San Diego, CA) with the exponential decay function to plot best-fit curves for the cell survival data. *t* Tests were performed to compare each test set with the melphalan alone-treated samples.

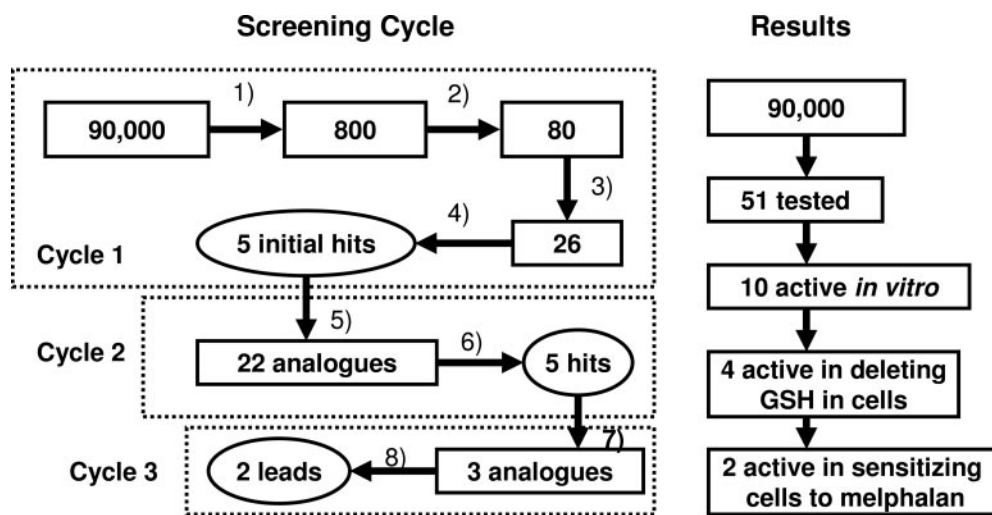
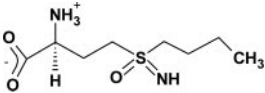
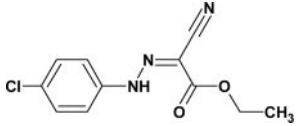
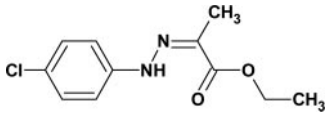
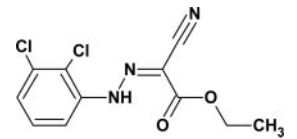
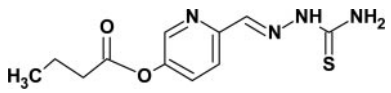
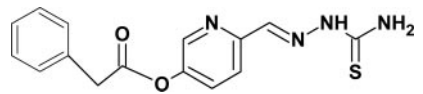
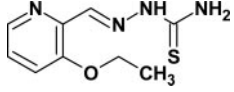
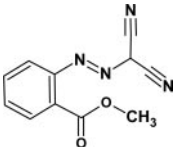
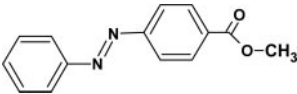
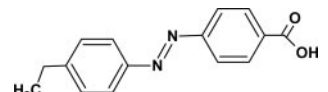
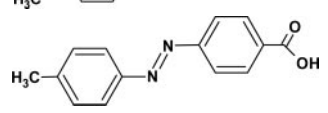
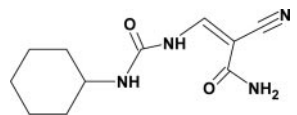
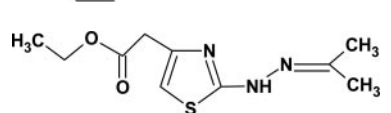


Fig. 2. Left, the three screening cycles. Right, the overall result of the screenings. Cycle 1 is receptor-based, using the γ -GCS_H molecular model as "bait" in virtual screening, whereas cycles 2 and 3 are ligand-based, testing compounds in vitro for γ -GCS_H inhibition or cellular GSH depletion. Notes for each cycle of the screenings are as follows: 1) using GOLD software, library screen setting; 2) GOLD, standard setting; 3) visual inspections to reduce the 80 compounds to 49 candidates after excluding compounds containing fewer than two polar atoms (N, O, S). Of the 49 compounds, 26 chemical samples were obtained from NCI; 4) enzymatic assays using recombinant human γ -GCS; 5) analogs of the initial hits in cycle 1 using the ANALOG algorithm; 6) enzymatic assays and cell-based GSH deletion assays; 7) analogs of the hits in cycle 2; and 8) assays to determine whether the compound could sensitize drug-resistant tumor cells to the treatment of melphalan, which were performed for all of the hits from each cycle.

TABLE 1

Chemical structures, K_i values, and the percentages of GSH decrease of the hits in cycles 1 to 3Binding studies used a coupled biochemical reaction, as described previously (Meister and Anderson, 1983), in which ADP formation was coupled to NADH oxidation. Decrease in GSH levels after incubation of A549 cells with compounds at 50 and 100 μ M concentrations is expressed as a percentage.

	NSC	Structure	K_i	Decrease in GSH Levels	
				50 μ M	100 μ M
			μ M	%	
L-BSO			151.3 \pm 43	90	90
Family A Cycle 1	176283		1420 \pm 153	—	—
Cycle 2	21429		66.7 \pm 27	—	—
	176282		380.9 \pm 104	—	—
Family B Cycle 1	185050		647.1 \pm 44	—	—
Cycle 2	266746		149.1 \pm 51	—	—
	104960		189.2 \pm 38	21	32
Family C Cycle 1	25809		1350 \pm 61	—	—
Cycle 2	118657		N.D.	—	—
Cycle 3	79068		N.D.	—	—
	59492		N.D.	—	—
Other Cycle 1	24196		414.0 \pm 52	—	—
	299962		325.3 \pm 94	—	—

N.D., not determined; —, inactive.

Recombinant Protein Production. The complete cDNA sequence for γ -GCS_H was kindly provided by Dr. Tim Mulcahy (University of Wisconsin, Madison, WI). The γ -GCS_H cDNA coding sequence was cloned into pet15b (Novagen, Madison, WI), and wild-type γ -GCS_H protein was expressed, purified, and quantified as described previously (Hamilton et al., 2003).

Inhibitor Activity Measurement. Binding studies used a coupled biochemical reaction in which ADP formation is coupled to NADH oxidation as described previously (Wu et al., 2001; Hamilton et al., 2003). For inhibitor K_i kinetic measurements, compounds were resuspended in DMSO and preincubated with the purified γ -GCS_H enzyme for 10 min at 37°C before adding to the reaction buffer. Reduction in absorbance of NADH at 340 nm and 37°C was followed over time using a 96-well plate microplate spectrophotometer (Benchmark Plus; Bio-Rad Laboratories, Hercules, CA). As control, reactions were also performed in complete buffer without γ -GCS protein. In addition, to ensure that the compounds did not directly interact with lactate dehydrogenase or pyruvate kinase, phosphate production was also measured as a means of monitoring activity after the protocol of Kyaw et al. (1985). Reactions also were performed on native enzyme without compound. Reaction blanks consisted of buffer plus enzyme but without NADH. Assays were performed in triplicate, and data were analyzed using a competitive inhibition model analysis. All analyses were performed using Sigma Plot 8.02 software (SPSS Inc., Chicago, IL).

For GSH depletion studies, 2×10^5 A549 cells were seeded in 60-mm dishes and allowed to attach overnight. Twenty-four hours later, fresh media containing test compounds dissolved in DMSO were added. All compounds were used at subcytotoxic doses. After incubation for 24 to 48 h, cells were washed, harvested, and assayed for GSH. As control, nontreated DMSO- and L-BSO-treated cells were used.

Glutathione Measurement. Intracellular GSH was measured using the enzymatic-recycling assay (Meister and Anderson, 1983). Absorbance was read at 405 nm in a 96-well plate format using an ELX800 microplate reader (Bio-Tek Instruments Inc.), and concentrations were determined using purified GSH as standard and expressed as nanomoles of GSH per milligram of protein. Protein concentrations were determined using the BCA Protein Assay Kit (Pierce Inc., Rockford, IL).

Comparison of the 3D Model of Human γ -GCS with the Crystal Structure of *E. coli* γ -GCS. When this work was initiated, there was no crystal of γ -GCS available. Extensive database searches for human γ -GCS_H using PSI-BLAST did not detect any homologous proteins with known structures. Therefore, we used a fold-recognition method to identify a structure template and built a 3D model of human γ -GCS_H (Hamilton et al., 2003). The template we identified is the crystal structure of glutamyl-tRNA synthetase (Protein Database entry, 1gln), which is an oxygen-nitrogen ligase, linking glutamyl to the 3'-OH of the tRNA terminal adenosine. Thus, we used an oxygen-nitrogen ligase as a structural template for a carbon-nitrogen ligase (γ -GCS_H). This is supported by the observation of Russell and Sternberg (1997) that glutamyl-tRNA synthetase shares a similar fold with one domain of glutamine synthetase, a carbon-nitrogen ligase. In the present work, based on the 3D model of human γ -GCS_H, we identified a series of novel compounds active in inhibiting human γ -GCS, which demonstrates that this 3D model is useful for virtual screening of human γ -GCS inhibitors.

Hibi et al. (2004) recently published the crystal structure of *E. coli* γ -GCS. However, there is no significant homology between *E. coli* and human γ -GCS, despite catalyzing similar reactions. The human γ -GCS is composed of a heavy subunit and a light subunit, in which the *E. coli* enzyme is a single 60-kDa polypeptide showing only 8% amino acid sequence identity with the human sequence. Studies of the substrate specificity of *E. coli* and mammalian γ -GCS have indicated that there are differences in the L-cysteine binding site, the rate-limiting amino acid in GSH synthesis (Lewandowicz et al., 2002). As such, it is not known how well the *E. coli* γ -GCS crystal

structure predicts the human homolog, and it has been suggested previously that *E. coli* and *Arabidopsis thaliana* γ -GCS proteins may have evolved independently from other species (May and Leaver, 1994).

On the other hand, L-BSO is a fairly potent inhibitor of both mammalian and *E. coli* γ -GCS (Griffith, 1982; Tokutake et al., 1998), suggesting that there are similarities in the binding sites of γ -GCS between species. However, by visual inspection, we did not identify significant similarity between the 3D model of human γ -GCS and the crystal structure of *E. coli* enzyme. This might be due to either some inaccuracy in the 3D model or structural species differences.

Results

Multiple-Cycle Screenings of the National Cancer Institute 3D Database. The NCI has a publicly available 3D chemical database that contains more than 200,000 compounds and consists of unique synthetic chemicals and natural products. Using the γ -GCS_H structural model we developed on the basis of biological data (Hamilton et al., 2003), we virtually screened 90,000 compounds from the NCI-3D database using the GOLD software and an ANALOG algorithm we developed as a functional module of the Hit Discovery platform. "Hit" compounds were physically obtained from the NCI and tested in biological assays. Any chemical structure that demonstrated GSH-depleting activity was used in subsequent cycles of virtual screening to further identify structural analogs (i.e., "guilty by similarity" strategy). The flow chart for the three screening cycles and the overall results are shown in Fig. 2. The chemical structures, K_i values, and the percentage of the GSH depletion for the hits of each cycle are reported in Table 1. The time-dependent enzymatic inhibition curves for selected compounds at various doses are shown in Fig. 3.

As shown in Fig. 2 and Table 1, the first cycle of screening led to the identification of five weak hits with the K_i values in the range of 325.3 to 1420 μ M. The K_i values reported here are the overall inhibition constants. The K_i value of L-BSO we obtained for the human γ -GCS is 151 μ M, whereas the K_i value of L-BSO for *E. coli* γ -GCS reported by Tokutake et al. (1998) was 49.3 μ M. Even though the hit compounds identified in cycle 1 demonstrated low potency inhibition against γ -GCS, we completed a second round of screening to look for further analogs. We identified a series of potent analogs of NSC176283, NSC185050, and NSC25809 in cycles 2 and 3 and classified these compounds into families A, B, and C, respectively (Table 1). Here, several particular points are worthy of note: 1) NSC21429 is more potent than L-BSO in enzymatic assays, but it is not active in depleting GSH in cellular assays. This could be due to differences in compound solubility, cell accumulation, or metabolism; 2) NSC104960 has a potency comparable with that of L-BSO in enzymatic assays, and more importantly, it is active in depleting GSH levels in A549 cells; 3) NSC118657, NSC79068, and NSC59492 showed considerable potency in decreasing GSH levels in A549 cells. However, because these three compounds are colored, which interfere with our enzymatic assays, we were unable to determine their K_i values; 4) overall, we identified four novel compounds active in depleting GSH in A549 cells, with NSC79068 being the most potent (Table 1); and 5) if we select the K_i value of NSC185050 (647.1 μ M) as the cutoff for active compounds and therefore consider NSC176283 and NSC25809 inactive, the total number of the

active compounds we identified was 10. In addition, we did not identify active compounds from the analogs of NSC24196 and NSC299962 that we obtained from NCI. But this cannot rule out other analogs of NSC24196 and NSC299962.

To investigate time-dependent inhibition profiles of the active compounds, the relative activities were plotted against time for selected compounds at various doses (Fig. 3). Inhibition of γ -GCS by L-BSO, NSC21429, NSC104960, and NSC185050 are clearly both time- and dose-dependent. At 500 μ M concentration, the time to reach 50% inhibition of the enzyme is approximately 8, 12, and 5 min for L-BSO, NSC21429, and NSC104960, respectively, whereas at 100 μ M, the time to reach the same extent of inhibition is approximately 27 and 17 min for L-BSO and NSC21429, respectively. Therefore, NSC21429 and NSC104960 showed faster binding kinetics than L-BSO at 100 and 500 μ M, respectively. In addition, compound NSC185050 is inactive at 100 μ M but inhibits the enzyme in time-dependent manner at 500 μ M. This supports the selection of NSC185050 as the cutoff for active compounds.

Compounds NSC59492 and NSC79068 Sensitize Tumor Cells to the Treatment of Melphalan. Melphalan is an alkylating chemotherapy agent for which elevated tumor GSH levels can help lead to drug resistance. Compound L-BSO depletes GSH and can reverse melphalan resistance

(Lewandowicz et al., 2002). For example, it was shown that L-BSO synergistically reverses melphalan resistance in a group of highly melphalan-resistant neuroblastoma cell lines (Meister and Anderson, 1983). To determine whether any of the novel γ -GCS inhibitors we identified could similarly sensitize tumor cells to melphalan treatment, we examined melphalan cytotoxicity in the presence of these compounds using L-BSO as a positive control. We used each compound's respective highest nontoxic dose as determined by toxicity studies. Figure 4 shows the results of cotreatment with melphalan in A549 cells. Pretreatment of cells with L-BSO results in 3.4-fold sensitization. NSC79068 or NSC59492 exposure resulted in smaller (1.5- and 1.4-fold, respectively) yet statistically significant decrease in the melphalan IC_{50} value.

Among the four novel compounds active in depleting cellular GSH (Table 1), NSC79068 and NSC59492 share the same skeleton, and both of them are active in sensitizing tumor cells to the treatment of melphalan. This suggests that structure family C represented by NSC79068 (Table 1) is a promising chemical class to be optimized as potent inhibitors of human γ -GCS, capable of enhanced chemosensitization. It is noteworthy that NSC104960 has a K_i value of 189.2 μ M and depleted the GSH level by 21% at 50 μ M concentration, but it is not active at sensitizing A549 cells to melphalan toxicity. This could be explained by its weak potency or the possibility

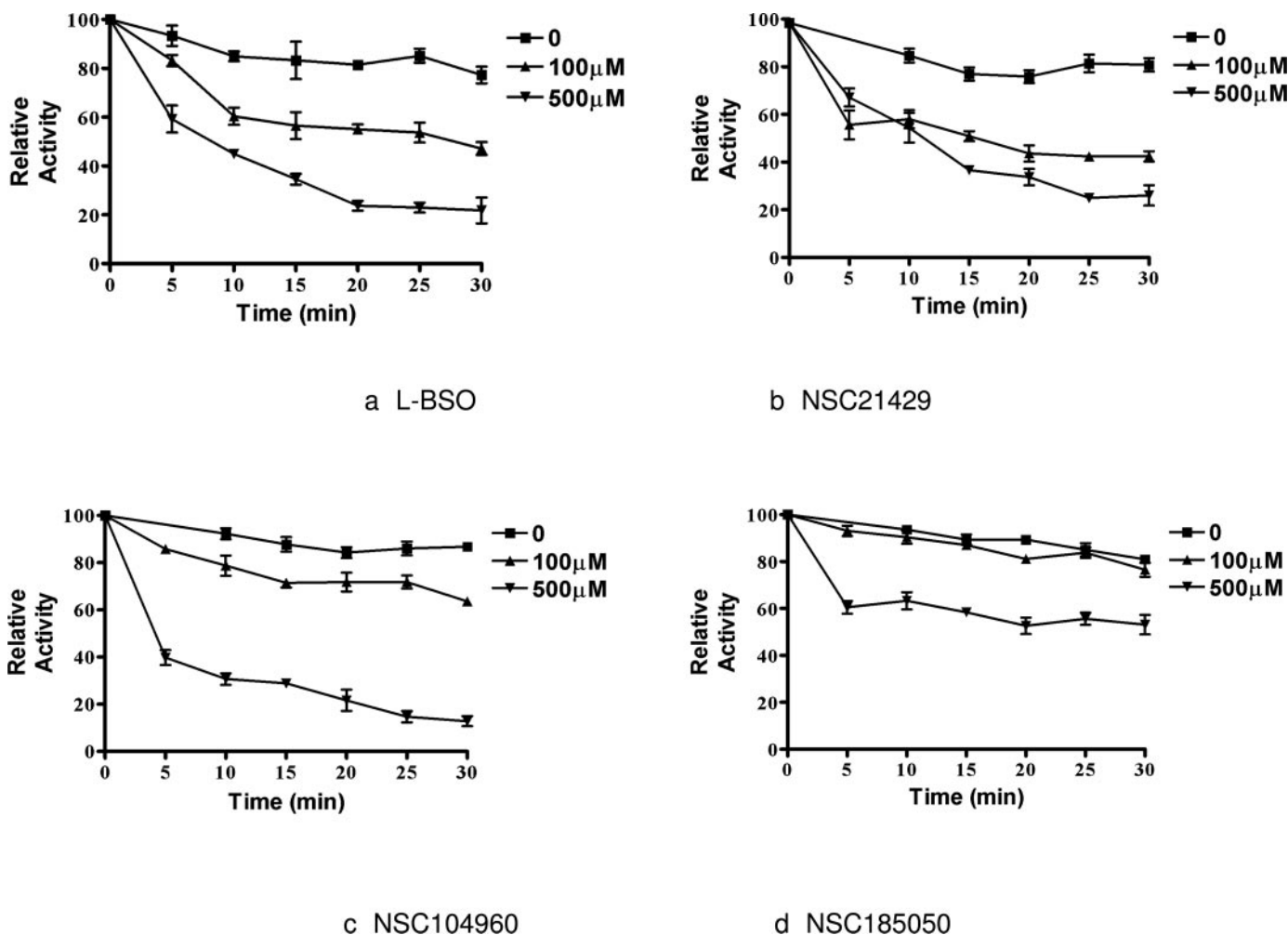


Fig. 3. Time-dependent inhibition curves for the selected active compounds at various concentrations. Relative activity is the enzyme activity over time of recombinant and purified γ -GCS_H.

of its being a reversible inhibitor. Consequently, structure class B represented by NSC104960 (Table 1) is another promising chemical class to be investigated further.

Comparison of the 3D Model of Human γ -GCS with the Crystal Structure of *E. coli* γ -GCS. To compare the performance of both structures in retrieving known active compounds from a virtual data set ($n = 200$), we first compiled a data set of 200 compounds, which is composed of L-S-BSO, the 10 active compounds we identified (Table 1), 39 inactive compounds that were identified by the enzymatic assays in this work, and 150 compounds that were randomly selected from the NCI database and assumed to be inactive. Next, using either the human 3D model or the crystal structure of *E. coli* γ -GCS, virtual screenings were performed to retrieve the active compounds from the data set, and the enrichment curves were plotted for two different GOLD default screen settings: library screen and standard setting (Fig. 5).

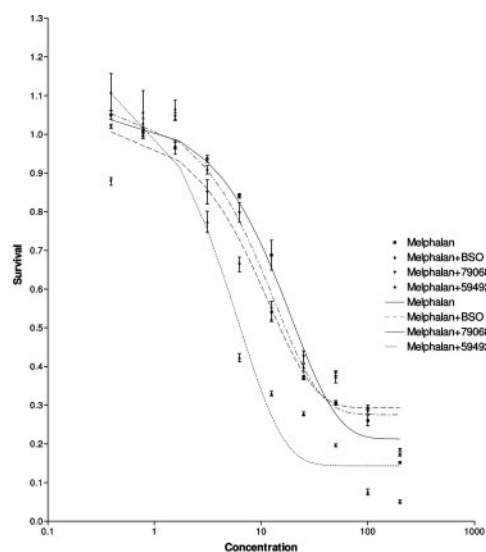
As shown in Fig. 5, the enrichment curves indicate that virtual screening using either the 3D model or the crystal structure of the enzyme are better than random selection at both GOLD screen settings. The 3D model of human γ -GCS is better than the crystal structure of *E. coli* enzyme in retrieving the compounds active against human γ -GCS (Fig. 5). This might reflect species differences at the enzymatic binding. For the 3D model, the top 10% of the data set ranked using GOLD standard setting (Fig. 5, bottom) was found to retrieve 50% of the active compounds, whereas the top 10% of the data set using library screen setting (Fig. 5, top) was shown to retrieve approximately 42% of the active compounds. Overall, the GOLD standard setting is considerably more

effective in retrieving the active compounds, although it is more computationally expensive than the library screen setting.

Discussion

Glutathione depletion remains a potentially important strategy for chemosensitization. Recent studies suggest that it may be particularly useful in MRP1-expressing cells (Rappa et al., 2003; Akan et al., 2005). Most of the preclinical studies used L-BSO as the GSH depleter, and initial clinical trials showed promise (Dwyer et al., 1996; Chen et al., 1998). However, the difficulty in synthesis of L-BSO has generated interest in identifying other GSH depleters. We are interested in finding entirely new chemical structures that can be used as GSH depleters.

By virtually screening the NCI-3D database using the structural model of human γ -GCS_H and the strategy to repeatedly search for the analogs of hit compounds, we identified 10 novel compounds active in inhibiting human γ -GCS. Among them, four compounds containing two novel classes of chemical skeletons were shown to deplete GSH levels in A549 tumor cells. Two compounds with related chemical skeletons also resulted in small but significant chemosensitization to melphalan. Although this effect is smaller than that of L-



	Melphalan	Melphalan+BSO	Melphalan+79068	Melphalan+59492
IC ₅₀	13.50	4.181	8.204	9.203
95% Confidence Intervals	16.04 to 11.65	5.255 to 3.472	11.82 to 6.281	11.45 to 7.694
P value		P<0.001	P<0.001	P<0.001

Fig. 4. Cell survival curves and calculated IC₅₀ values for A549 cells exposed to varying doses of melphalan \pm L-BSO, NSC59492, or NSC79068 at their respective highest nontoxic dose. Student's *t* test was used to compare each GSH depleter-treated test set with the melphalan alone-treated cells.

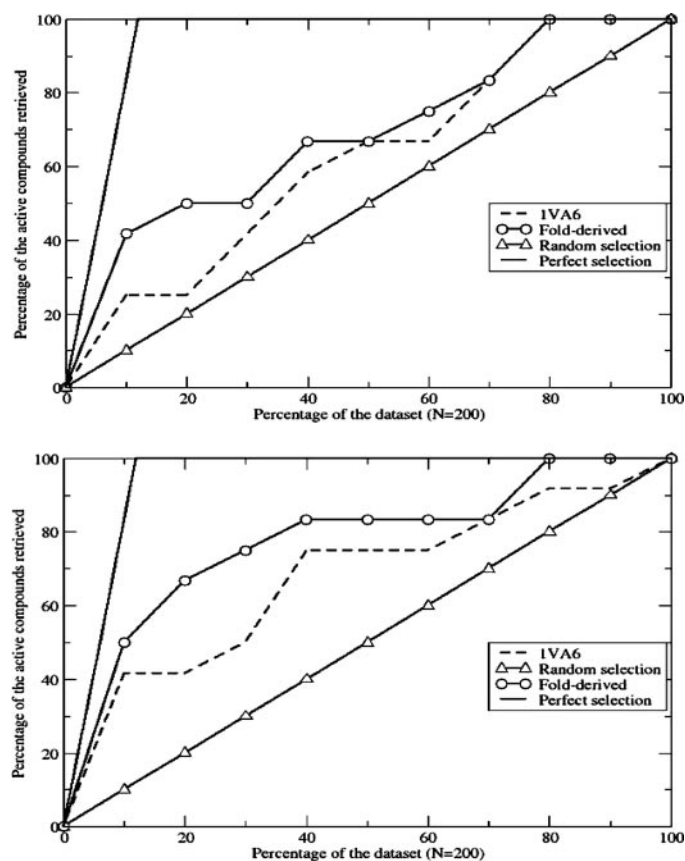


Fig. 5. Comparison of virtual screening performance by enrichment curves. The curves represent the percentage of inhibitors retrieved as a function of the percentage of total molecules in the data set ($n = 200$) for the 3D model of human γ -GCS (○) and IVA6, which is the crystal structure of *E. coli* γ -GCS (broken lines). The curves were constructed using two different virtual screening settings: top, GOLD library screen setting; bottom, GOLD standard setting. The curves for perfect selection (solid lines) and random selection (△) are shown.

BSO, we have nonetheless identified two promising chemical classes, represented by NSC79068 and NSC104960, which can now be further optimized as γ -GCS inhibitors using medicinal chemistry. This is the point at which issues of solubility and clinical delivery solvents will be addressed. In addition, we demonstrated that a 3D molecular model can be an effective tool in identifying potential chemical interactors using virtual screening.

Acknowledgments

We are grateful for the chemical samples as a gift from the Drug Synthesis and Chemistry Branch (Developmental Therapeutics Program, NCI, Bethesda, MD). We appreciate the helpful contribution of Andrew Bier.

References

- Akan I, Akan S, Akca H, Savas B, and Ozben T (2005) Multidrug resistance-associated protein 1 (MRP1) mediated vincristine resistance: effects of N-acetylcysteine and buthionine sulfoximine. *Cancer Cell Int* **5**:22.
- Chen X, Carystinos GD, and Batist G (1998) Potential for selective modulation of glutathione in cancer chemotherapy. *Chem Biol Interact* **112**:263–275.
- Davison K, Mann KK, Waxman S, and Miller WH Jr (2004) JNK activation is a mediator of arsenic trioxide-induced apoptosis in acute promyelocytic leukemia cells. *Blood* **103**:3496–3502.
- Dwyer PJ, Hamilton TC, LaCreta FP, Gallo JM, Kilpatrick D, Halbherr T, Brennan J, Bookman MA, Hoffman J, Young RC, et al. (1996) Phase I trial of buthionine sulfoximine in combination with melphalan in patients with cancer. *J Clin Oncol* **14**:249–256.
- Griffith OW (1982) Mechanism of action, metabolism, and toxicity of buthionine sulfoximine and its higher homologs, potent inhibitors of glutathione synthesis. *J Biol Chem* **257**:13704–13712.
- Griffith OW and Friedman HS (1991) Glutathione and resistance to anticancer therapies in *Synergism and Antagonism in Chemotherapy* (Chou TC, Rideout DC eds) pp 245–285, Academic Press, San Diego.
- Griffith OW and Mulcahy RT (1999) The enzymes of glutathione synthesis: gamma-glutamylcysteine synthetase. *Adv Enzymol Relat Areas Mol Biol* **73**:209–267.
- Hamilton D, Wu JH, Alaoui-Jamali M, and Batist G (2003) A novel missense mutation in the γ -glutamylcysteine synthetase catalytic subunit gene causes both decreased enzymatic activity and glutathione production. *Blood* **102**:725–730.
- Hibi T, Nii H, Nakatsu T, Kimura A, Kato H, Hiratake J, Oda J (2004) Crystal structure of gamma-glutamylcysteine synthetase: insights into the mechanism of catalysis by a key enzyme for glutathione homeostasis. *Proc Natl Acad Sci USA* **101**:15052–15057.
- Hiratake J, Irie T, Tokutake N, and Oda JI (2002) Recognition of a cysteine substrate by *E. coli* γ -glutamylcysteine synthetase probed by sulfoximine-based transition-state analogue inhibitors. *Biosci Biotechnol Biochem* **66**:1500–1514.
- Kyaw A, Maung-U K, and Toe T (1985) Determination of inorganic phosphate with molybdate and Triton X-100 without reduction. *Anal Biochem* **145**:230–234.
- Lewandowicz GM, Britt P, Elgie AW, Williamson CJ, Coley HM, Hall AG, and Sargent JM (2002) Cellular glutathione content, in vitro chemoresponse, and the effect of BSO modulation in samples derived from patients with advanced ovarian cancer. *Gynecol Oncol* **85**:298–304.
- Lyne PD (2002) Structure-based virtual screening: an overview. *Drug Discovery Today* **7**:1047–1055.
- May MJ and Leaver CJ (1994) *Arabidopsis thaliana* γ -glutamylcysteine synthetase is structurally unrelated to mammalian, yeast, and *Escherichia coli* homologs. *Proc Natl Acad Sci USA* **91**:10059–10063.
- Meister A (1989) Metabolism and function of glutathione, in *Glutathione: Chemistry, Biochemical and Medical Aspects* (Dolphin D, Avramovich A, Poulson R eds) pp 367–474, John Wiley & Sons, Inc., New York.
- Meister A and Anderson ME (1983) Glutathione metabolism and function. *Annu Rev Biochem* **52**:711–760.
- Perola E, Xu K, Kollmeyer TM, Kaufmann SH, Prendergast FG, and Pang YP (2000) Successful virtual screening of a chemical database for Farnesyltransferase inhibitor leads. *J Med Chem* **43**:401.
- Ramanathan B, Jan KY, Chen CH, Hour TC, Yu HJ, and Pu YS (2005) Resistance to paclitaxel is proportional to cellular total antioxidant capacity. *Cancer Res* **65**:8455–8460.
- Rappa G, Gamcsik MP, Mitina RL, Baum C, Fodstad O, and Lorico A (2003) Retroviral transfer of MRP1 and gamma-glutamyl cysteine synthetase modulates cell sensitivity to L-buthionine-S,R-sulphoximine (BSO): new rationale for the use of BSO in cancer therapy. *Eur J Cancer* **39**:120–128.
- Russell RB and Sternberg MJ (1997) Two new examples of protein structural similarities within the structure-function twilight zone. *Protein Eng* **10**:333–338.
- Tokutake N, Hiratake J, Katoh M, Irie T, Kato H, and Oda JI (1998) Design, synthesis and evaluation of transition-state analogue inhibitors of *Escherichia coli* γ -glutamylcysteine synthetase. *Bioorg Med Chem* **6**:1935–1953.
- Torky AR, Stehfest E, Viehweger K, Taege C, and Foth H (2005) Immunohistochemical detection of MRPs in human lung cells in culture. *Toxicology* **207**:437–450.
- Wu JH, Batist G, and Zamir LO (2001) Identification of a novel steroid derivative, NSC12983, as a Paclitaxel-like tubulin assembly promoter by 3-D virtual screening. *Anticancer Drug Des* **16**:129–133.
- Yoshida A, Takemura H, Inoue H, Miyashita T, and Ueda T (2006) Inhibition of glutathione synthesis overcomes Bcl-2-mediated topoisomerase inhibitor resistance and induces nonapoptotic cell death via mitochondrial-independent pathway. *Cancer Res* **66**:5772–5780.
- Zhu XH, Shen YL, Jing YK, Cai X, Jia PM, Huang Y, Tang W, Shi GY, Sun YP, Dai J, et al. (1999) Apoptosis and growth inhibition in malignant lymphocytes after treatment with arsenic trioxide at clinically achievable concentrations. *J Natl Cancer Inst* **91**:743–745.

Address correspondence to: Dr. Gerald Batist, Segal Cancer Centre and Lady Davis Institute for Medical Research, Sir Mortimer B. Davis-Jewish General Hospital, 3755 Cote-Ste-Catherine Road, Montreal, QC, Canada, H3T 1E2. E-mail: gbatist@onc.jgh.mcgill.ca